Modelling spatiotemporal gradients of biomolecules on polyethylene glycol hydrogels

Author: Jordi Folch Eguren
*Facultat de Física, Universitat de Barcelona, Diagonal 645, 08028 Barcelona, Spain.**

Advisors: Elena Martínez, Gizem Altay

Abstract: The diffusion of the stemness proteins Epidermal grow factor, R-spondin and Noggin (involved in the intestinal epithelial development) within a hydrogel material was simulated using COMSOL Multiphysics software. For the model, similar sized model proteins; Insulin, Carbonic Anhydrase and Bovine Serum Albumin were used. The steady state times and concentrations were determined at the gel surface for a rectangular and a pillar array model. It has been found that geometry was important and had to be implemented in order to better predict the surface concentrations. The gradient obtained along the pillar surface was most evident for BSA (Noggin). We believe that this model can be useful in designing experiments in intestinal epithelial development studies.

I. INTRODUCTION

Biomolecular gradients control many important biological processes such as tissue development [1], migration of immune cells [2], and cancer metastasis [3]. One of such biological processes takes place in the intestinal epithelium. The intestinal epithelium is continuously renewed due to the presence of intestinal stem cells (ISCs). ISCs reside within the crypts of the crypt-villi units of the intestinal epithelium (Fig.1A) [4] and the progeny of these cells migrate up along the villi and differentiate into absorptive and secretory cells [4]. This process is tightly controlled by the gradients of the effectors of the Wnt, bone morphogenic protein (BMP), and epidermal growth factor (EGF) signaling pathways (Fig.1B).

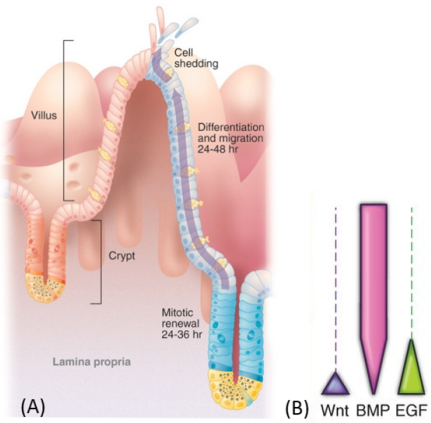

FIG. 1: (A) Diagram showing the crypt-villi unit of the intestinal epithelium (*http : //www.ufrgs.br/imunovet/molecular − immunology/gastrointestinal.html*). (B) Scheme showing the spatial gradients of Wnt, BMP, and EGF signals that are formed along the crypt axis [4].

*Electronic address: jofoeg@gmail.com

In our group, we have previously developed a polyethylene glycol diacrylate (PEGDA) hydrogel based villi-like 3D scaffolds that supported the growth of ISCs. In order to control the growth, migration and differentiation of ISCs we aimed at forming stable spatial gradients of Wnt, BMP and EGF signals on PEGDA hydrogels. In this project, our objective was to model these gradients on hydrogels using finite element analysis (FEM) through COMSOL Multiphysics® software.

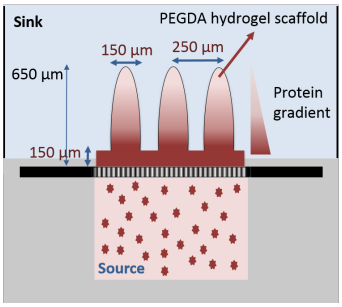

FIG. 2: Scheme showing the experimental setup

Stemness factor	Molecular mass (kDa)	Model protein	Molecular mass (kDa)
EGF	6.0	Insulin	5.7
R-spondin	27.0	CA	28.0
Noggin	46.4	BSA	66.5

TABLE I: Stemness factors and their corresponding model proteins with their molecular mass.

In the experimental setup the gradient is created using a source chamber located at the bottom of the villi-like 3D hydrogel scaffolds and a sink chamber at the top (Fig.2). The stemness factors R-spondin (Wnt agonist), Noggin (BMP antagonist) and EGF were added to the source chamber. BMP antagonist, Noggin, was used since the BMP gradient direction is opposite to the source

(Exp fig). For the FEM simulation, however, model proteins with similar sizes were used (Table I), since we can readily find the values for hydrodynamic radius and diffusion coefficients of these model proteins in the literature.

II. FICK'S LAW

The diffusion of proteins can be described by Fick's second law:

$$\frac{\partial c}{\partial t} = D\nabla^2 c \tag{1}$$

Where c is the protein concentration as a function of time and space, and D is the diffusion coefficient. By using this equation we are making some assumptions: D is a constant value, there are no chemical reactions, there is no convection, the specie c is diluted and there is mass conservation. The diffusion coefficient of proteins in solution, D_0, can be calculated using Stokes-Einstein equation for diffusion of a spherical particle through a liquid:

$$D_0 = \frac{k_B T}{6\pi\eta r} \tag{2}$$

Where k_B is the Boltzmann's constant, T is the absolute temperature, η is the viscosity of the solvent and r is the protein hydrodynamic radius. Calculated D_0 values represent the diffusion coefficient of a sphere with an equivalent size.

III. COMSOL MODEL

For simulations, the 'Transport of diluted species' module of Comsol Multiphysics® software was used. We assumed axial symmetry and that made it possible to reduce the 3D forms to 2D geometries. The geometry was composed of two media; the PEGDA hydrogel and the aqueous solution. For each medium the corresponding diffusion coefficient values (i.e. D_0 for aqueous solution, D_g for PEGDA hydrogel) was used (Table II). A constant source concentration (Table II) is put at the bottom boundary of the gel and no flux boundary is selected for the rest of the boundaries found at the edges of the geometry. At these boundaries of the aqueous medium the initial concentration was set to zero.

First, we started with simplified rectangular forms. We did simulations for two different PEGDA gel heights 150 μm (corresponding to the base height of the pillar forms) and 650 μm (corresponding to the pillar height). In the second model, we implemented the pillar geometry with a base height of 150 μm, and the pillars with a semi-major axis of 75 μm (half-width) and a semi-minor axis of 500 μm (height) being considered as semi ellipses (Fig.2).

Protein	Radius (nm)	D_0 (m/s^2)	D_g (m/s^2)	Concentration (mol/m^3)
Insulin	1.50 [5]	$2.19 \cdot 10^{-10}$	$1.27 \cdot 10^{-10}$ [5]	$1.75 \cdot 10^{-5}$
CA	2.40 [5]	$1.37 \cdot 10^{-10}$	$1.60 \cdot 10^{-11}$ [5]	$3.45 \cdot 10^{-6}$
BSA	3.60 [6]	$9.10 \cdot 10^{-11}$	$1.27 \cdot 10^{-11}$ [7]	$1.50 \cdot 10^{-6}$

TABLE II: Values for the hydrodynamic radius of the model proteins; the diffusion coefficients in the aqueous solution at 37°C, D_0, calculated with Eqn. (2); diffusion coefficients in the PEGDA gel, D_g; and the source concentrations for each protein.

The center-to-center spacing was set to 250 μm and an array of pillars were constructed. The aim of doing these two models was to understand the effect of the geometric form. The mesh for the aqueous media was set to finer in both models and the mesh for the gel media was improved at the edges. The objective was to find the steady state (the point after which the concentration doesn't evolve with time) for each protein and the corresponding surface concentrations. For the pillars model, we wanted to find the concentration as a function of the position along the pillar surface to be able to determine if those concentrations were sufficient to guide ISCs growth and differentiation. At steady state, we expected to obtain a line graph, and indeed, if we set that c does not evolve with time in Eqn. (1), the differential equation solution becomes a line.

IV. RESULTS AND DISCUSSION

In order to determine the steady state at the surface of the gel we plot the concentration as a function of time for a point situated at the gel - aqueous solution interface for the rectangular models (h: 0.01 x $1.50 \cdot 10^{-4}$ m and h: 0.01 x $6.50 \cdot 10^{-4}$ m) (Fig.3, Fig.4). For the pillars we have chosen three points: at the gel - aqueous solution interface (h: 0.01 x $1.50 \cdot 10^{-4}$ m), at the interior of the pillar (h: 0.01 x $1.50 \cdot 10^{-4}$ m) and at the pillar tip (h: 0.01 x $6.50 \cdot 10^{-4}$ m) (Fig.5). Note that the source concentrations are different for each protein; therefore, diffusion times should be evaluated separately (source concentrations were set to minimum necessary concentrations for the ISCs growth). However, it has been checked that when the source concentrations were the same, the first protein to reach the steady state was Insulin, followed by CA and BSA (data not shown), as $D_{Insulin} > D_{CA} > D_{BSA}$.

For the rectangular models (Fig.3, Fig.4) the steady state times and corresponding concentrations for Insulin, CA and BSA are presented in Table III. We see that, as expected, the proteins reach the steady state earlier in the 150 μm height model with higher concentrations due to their proximity to the source. It has also found that at steady state the concentrations along a horizantal line within the gel media was constant (independent of hor-

izontal position), implying that there was only vertical diffusion in rectangular models (data not shown). As a general trend BSA arrived the steady state earliest, then the CA and Insulin latest. A possible explanation to this could be that although $D_{Insulin} > D_{CA} > D_{BSA}$, the source concentrations (Table II) are as follows; $c_{Ins} > c_{CA} > c_{BSA}$.

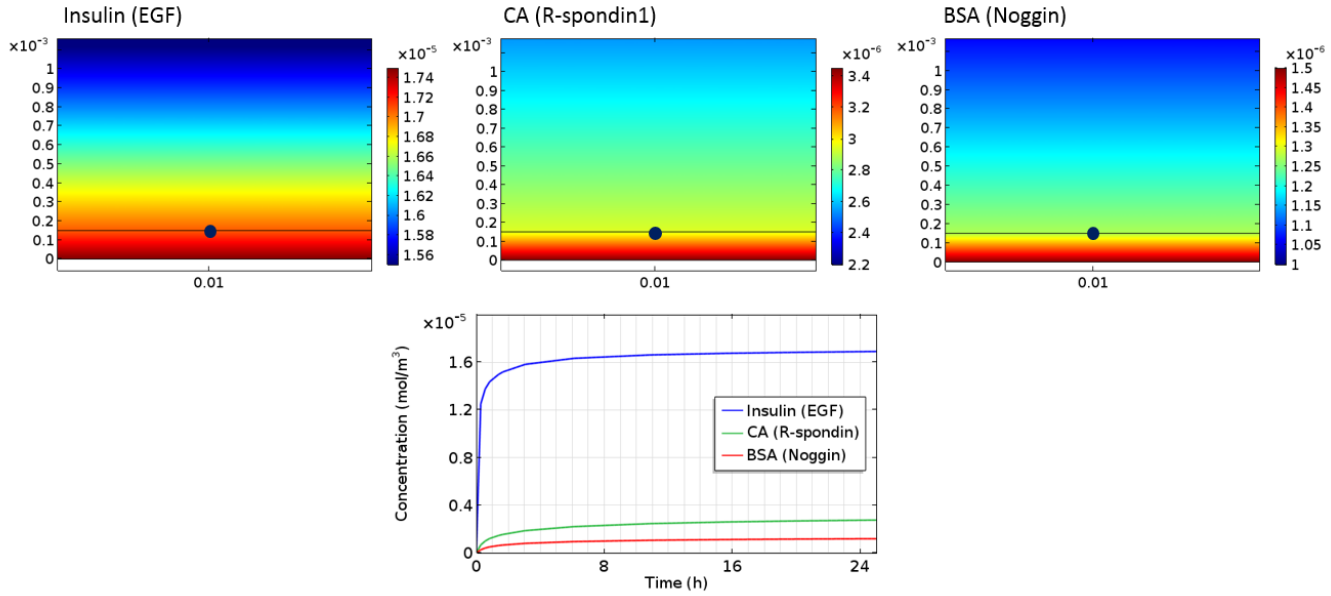

FIG. 3: Results from the 2D FEM simulations of the rectangle model (0.01 x $1.50 \cdot 10^{-4}$ m) for Insulin, CA and BSA at steady state. The height of the rectangle corresponds to the base height of the pillar model. Graph showing how the concentrations of the proteins change with time at a point at the interface (represented by the black dot in the solutions).

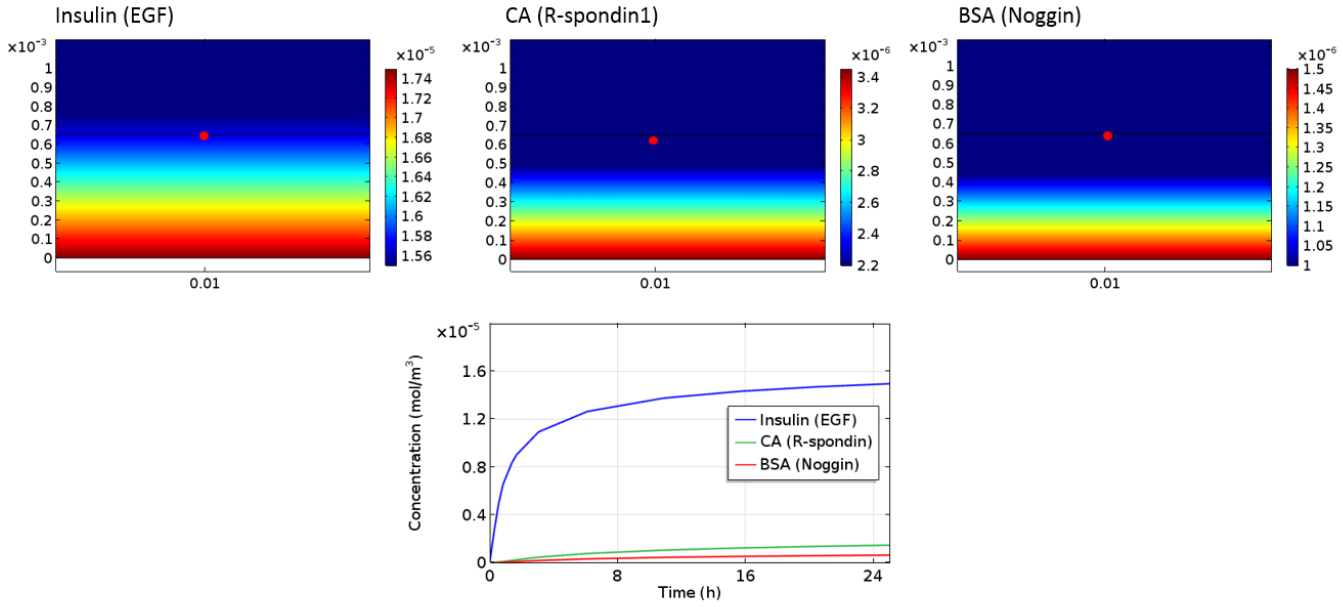

FIG. 4: Results from the 2D FEM simulations of the rectangle model (0,01 x $6.50 \cdot 10^{-4}$ m) for Insulin, CA and BSA at steady state. The height of the rectangle corresponds to the pillar height of the pillar model. Graph showing how the concentrations of the proteins change with time at a point at the interface (represented by the red dot in the solutions).

For the pillar model we have determined the steady state times and the concentrations at three different

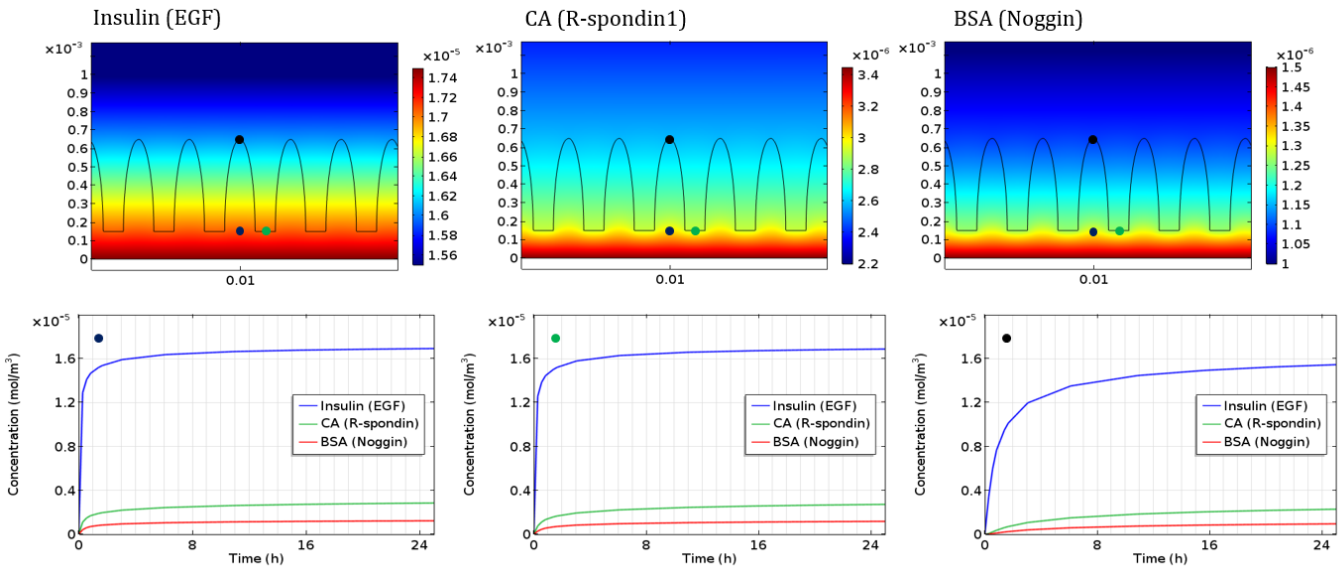

FIG. 5: Results from the 2D FEM simulations of the pillar model for Insulin, CA and BSA at steady state. Graph showing how the concentrations of the proteins change with time at three different points; at the base at the interface (represented by green dots in the solutions), at the base height inside the pillar (represented by blue dots in the solutions), and at the pillar tip (represented by black dots in the solutions).

Protein	c_{150} (mol/m^3)	t_{150} (h)	c_{650} (mol/m^3)	t_{650} (h)
Insulin	$1.71 \cdot 10^{-5}$	32	$1.59 \cdot 10^{-5}$	64
CA	$2.80 \cdot 10^{-6}$	30	$2.03 \cdot 10^{-6}$	56
BSA	$1.09 \cdot 10^{-6}$	14	$8.68 \cdot 10^{-7}$	30

TABLE III: Steady state times and corresponding concentrations for each protein for the rectangular models at 150 μm and 650 μm height. The values were calculated from the graphs and should be considered as approximates.

points; at the base at the gel-aqueous solution interface (green dots), at the base height inside the pillar (blue dots), and at the pillar tip (black dots) (Fig.5). For the points at the base height (i.e. 150 μm), although all the proteins have reached the steady state at the same time (24 h for Insulin, 16 h for CA and 10 h for BSA), the equilibrium concentrations were slightly different depending on the position; inside the pillar $1.71 \cdot 10^{-5}$ mol/mol^3 for Insulin, $2.85 \cdot 10^{-6}$ mol/mol^3 for CA, and $1.23 \cdot 10^{-6}$ mol/mol^3 for BSA and at the interface $1.71 \cdot 10^{-5}$ mol/mol^3 for Insulin, $2.72 \cdot 10^{-6}$ mol/mol^3 for CA, and $1.18 \cdot 10^{-6}$ mol/mol^3 for BSA. Lower steady state concentrations at the interface can be explained by more rapid diffusion of the proteins due to increased diffusion coefficients from the gel to the aqueous media. However, from the biological point of view these differences are insignificant; therefore, we can consider these points equivalent. It has found that the concentration values at the interface that listed above and the ones of the rectangular model with the 150 μm height (Table III), are quite close. Also, looking at the graphs of the 150 μm height rectangular model (Fig.3) and that of the point at the base height at the interface of the pillar model (Fig.5) similar behaviours are observed.

Protein	Steady state (h)	Concentration (mol/m^3)
Insulin	80	$1.65 \cdot 10^{-5}$
CA	70	$2.80 \cdot 10^{-6}$
BSA	48	$1.20 \cdot 10^{-6}$

TABLE IV: Steady state times and corresponding concentrations for each protein at the tip of the pillar.The values were calculated from the graphs and should be considered as approximates.

For the point at the tip of the pillar (black dot) we have also determined the steady state times and corresponding concentrations (Table IV). Comparing with the 650 μm height rectangular model (Fig.4), all the proteins had greater steady state times and therefore higher concentrations. This discrepancy between the rectangular and the pillar model can be explained by the geometry. In the pillar model there is more surface area for the proteins to escape to the aqueous media, so more time is needed to arrive to the steady state; and consequently, the concentrations will be greater. It has also been found that there was horizontal diffusion; however, it was negligible (data not shown). We have also determined the concentration as a function of position along the pillar surface for the

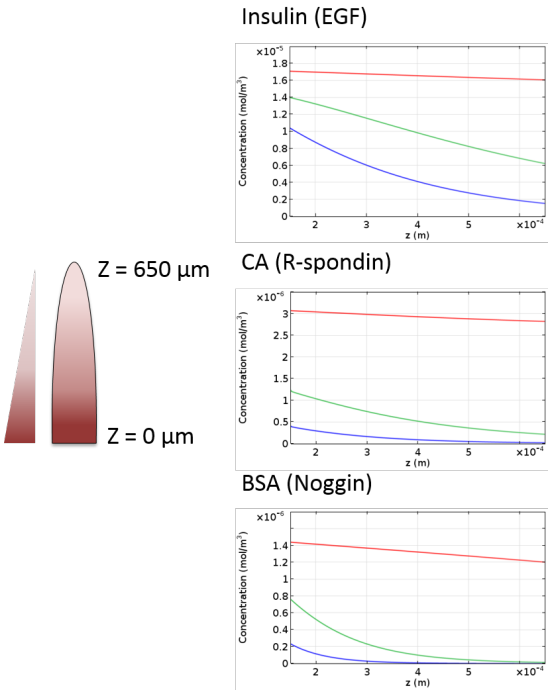

FIG. 6: Concentrations as a function of position along the surface of one pillar at 500 s, 1000 s, and at the steady state (for 650 μm height in the pillar model); represented by blue, green, and red lines, respectively.

three proteins (Fig.6). Before arrive to the steady state we observe the decay along the z axis, with increased times the lines become more linear. Finally, when the steady state is reached straight lines are obtained as dictated by the Eqn (1). The most marked gradient was that of BSA (Noggin), followed by CA (R-spondin) and Insulin (EGF) being insignificant.

V. CONCLUSIONS

We have modelled the diffusion of the stemness proteins involved in the development of the intestinal epithelium with the Comsol Multiphysics program using the diffusion coefficients of the similar sized model proteins; Insulin, CA and BSA. By plotting the concentration as a function of the time we have determined the steady state times and corresponding concentrations. We found that for all scenarios Insulin had reached the steady state latest, followed by CA and BSA. This can be explained by higher source concentration of Insulin compared to CA and BSA. In the pillar model we have found that the point at the base height at the gel-aqueous solution interface, and at the base height inside the pillar were equivalent. They were also equivalent to the corresponding point in the 150 μm height rectangular model. When we compared points at the interface for 650 μm height in the rectangular and pillar model we have found discrepancies in steady state times and concentrations. This can be attributed to the geometry. Therefore, complex geometries of the scaffolds have to be implemented into the model, in order to better predict the gradients. We have also determined the concentrations as a function of position along the pillar surface. The most marked gradient was that of BSA (Noggin), followed by CA (R-spondin) and Insulin (EGF) being insignificant. The source concentrations used in the model (Table II) are the ones that are routinely used for the maintenance of stemness of ISCs in culture [8]. And it was hypothesized that the gradients of these stemness factors would control ISCs migration and differentiation to form the intestinal epithelium in culture. Whether these gradients can lead the ISCs migration and differentiation should be tested experimentally. Depending on the experimental results model can be modified for better experimental outputs. In this iterative way, using both the experimental data and the simulation, it will be possible to control the growth, migration and differentiation of ISCs.

Acknowledgments

I would like to express my gratitude to my supervisors Dr. Elena Martínez and Gizem Altay who have directed my work. Also I would like to thank to all the members of Biomimetic systems for cell engineering group at IBEC, especially to Enara Larrañaga and Maria Valls for their help. Also, my special gratitude is for René Lázaro who has solved my problems and doubts about the Comsol program.

[1] Weijer, C.J. *J.Cell Sci*, 122(18) : 3215-23, 2009.
[2] Sip, C.G., Bhattacharjee, N. & Folch, A., *Lab chip*, 14(2), 302-14, jan 2014.
[3] Roussos, E.T., Condeelis, J.S. & Patsialou, A., *Nat. Rev. Cancer*, 11(8), 573-87, jan 2011.
[4] Sato, T. & Clevers, H., *Science*, 340(6137) : 1190-4, jun 2013.
[5] Weber, L.M., Lopez. C.G. & Anseth, K.S., *J.Biomed. Mater. Res. Part A*, 90(3): 720-729, sept 2009.
[6] Koutsopoulos, S., Unsworth, L.D., Nagai, Y. & Zhang, S., *PNAS*, 106: 4623-8, 2009.
[7] Altay, G., *Engineering a Platform for the Basic Research of Migration and Differentiation of Intestinal Stem Cells*, PhD follow-up committee report, University of Barcelona, 2015.
[8] Yin, X., Farin, H. F., H van Es, J., Clevers, H., Langer, R. & Karp, J. M., *Nat. Methods*, 11(1): 106-12, dec 2013.